

# Total Quadrant Security Region for Active Distribution Network with High Penetration of Distributed Generation

Jun Xiao, *Member, IEEE*, Guoqiang Zu, Huan Zhou, and Xinsong Zhang

**Abstract**—The region-based method has been applied in transmission systems and traditional passive distribution systems without power sources. This paper proposes the model of total quadrant security region (TQSR) for active distribution networks (ADN) with high penetration of distributed generation (DG). Firstly, TQSR is defined as a closed set of all the  $N-1$  secure operation points in the state space of ADN. Then, the TQSR is modeled considering the constraints of state space, normal operation and  $N-1$  security criterion. Then, the characteristics of TQSR are observed and analyzed on the test systems with different DG penetrations. TQSR can be located in any quadrant of the state space. For different DG penetrations, the shape and security features of TQSR are also different. Finally, the region map is discovered, which summarizes the features of different types of distribution networks.

**Index Terms**—Active distribution network (ADN), total quadrant security region (TQSR),  $N-1$  security, distributed generation (DG), region map.

## I. INTRODUCTION

THE future distribution network, especially in the urban area, will develop as an active system, which is able to dynamically select economic and reliable operation mode according to the consecutive changes caused by external environment such as load fluctuations, intermittent distributed generation (DG) and demand response (DR) [1], [2]. Active distribution network (ADN) [3] is a new operation mode for distribution networks for integrating high penetration DGs.

The most basic scientific problems for investigating a system include describing the maximum range of the system and determining the related maximum output. The research on transmission networks is mature. However, the security problem is not applicable to distribution networks. In a distri-

bution network and under any single contingency, reliable power supplies should be maintained for the areas without a fault within operation limits. For ADN with DGs, the security and efficiency of distribution networks become more complicated. At present, with the help of advanced secondary equipment of ADN, real-time monitoring and security assessment for ADN can be realized. However, the existing security assessment is based on case-by-case simulation approach [4], which is time-consuming and cannot provide effective quantitative indices. Meanwhile, it cannot meet the requirement of security assessment for ADN. Therefore, it is an urgent problem to study the ADN model including DGs and explore a faster approach to obtain the security boundary, which can provide a guidance to reveal the security characteristics of power grid, improve the efficiency of distribution network, and observe the nature and the defect of the power grid.

Distribution system security region (DSSR) is a new approach for the security analysis and assessment of distribution systems. DSSR is defined as a closed set of all the  $N-1$  secure operation points [5], whose boundary is usually expressed by hyperplanes. In actual operation, each system state corresponds to an operation point, which uniquely determines the system security status. Compared with the conventional case-by-case simulation approach, the region-based approach presents the global information about the security boundary surrounding the operation point of the system and the security margin to stability and operation limits [6]. This method provides a new security assessment approach for the operation of future smart distribution system and its effectiveness has been demonstrated [5]. The complicated operation boundary can be approximately expressed by simple hyperplanes, which benefits the optimization problem [7] and probabilistic assessment [8], especially for ADN with uncertainties due to intermittent DGs. A mathematical model of DSSR is established [5], [9] and the related approximation approach is proposed based on  $N-1$  simulation in searching the boundary of DSSR [10], which enables DSSR to be visualized in 2-dimension (2D) or 3-dimension space. Meanwhile, relevant researches explore the characteristics of DSSR [10], [11]. The application value of DSSR is excavated, providing the information of security margin and optimal control via the relative location of the operation point to each boundary. With real-time measurements to locate the

Manuscript received: November 4, 2018; accepted: March 13, 2020. Date of CrossCheck: March 13, 2020. Date of online publication: October 6, 2020.

This work was supported in part by National Key Research and Development Program of China (No. 2016YFB0900100), National Natural Science Foundation of China (No. 51877144), and China Postdoctoral Science Foundation (No. 2020M670668).

J. Xiao and H. Zhou (corresponding author) are with the School of Electrical Engineering, Tianjin University, Tianjin, China (e-mail: xiaojun@tju.edu.cn; huanzhou@tju.edu.cn).

G. Zu is with the State Grid Tianjin Electric Power Research Institute, Tianjin, China (e-mail: zuguoqiang\_tju@163.com).

X. Zhang is with the School of Electrical Engineering, Nantong University, Nantong, China (e-mail: prettypebble@163.com).

DOI: 10.35833/MPCE.2018.000745



operation point, the region-based approach is convenient for operators to monitor the system and take preventive actions [12], [13]. DSSR related theories are of great significance to the planning and operation of distribution systems and have been also applied in a large number of cases. For instance, a new distribution management system (DMS) based on the security region is proposed and applied in [14]. In the application of distribution system planning, DSSR also has the related achievement [15]. In addition, the concept of DSSR is applied in other fields such as power electronics [16] and ship-board DC zonal electric distribution systems [17].

The existing researches on DSSR are all related to traditional distribution systems, including the definition [5], observation [10], model [5], [9], characteristics [10], [11] and application [14]. The function of the traditional distribution networks is to passively receive the energy from transmission networks and supply the energy to the loads. The traditional distribution network is called the load supply network (LSN) in this paper. However, ADN is a typical system with power sources like DGs, of which the power will both inject into and flow out of a bus, and the power flow of branches can be bidirectional. Thus, the function of ADN will be power supply and DG absorption. Because of the bidirectional power flow of ADN, it can be deduced that the security region of ADN will be expanded from only quadrant I to any quadrants of the state space, turning into the total quadrant security region (TQSR). TQSR is defined as a closed set of all the  $N-1$  secure operation points for ADN, and it is an extension of DSSR in ADN. However, the technical gap is that there is a possibility of bidirectional power flow in ADN, and the problems of reverse power flow and over-voltage need to be considered. Thus, when observing the 2D security region of ADN, it is found that the security region appears in four quadrants, which is a new change. Therefore, the model and characteristics of the region will also be changed greatly and a new region theory for ADN is needed. There have been studies on ADN security [18], and this paper will conduct reasonable modeling and in-depth discussion from the perspective of the region.

The contributions of this paper are as follows. It proposes the concept and model of TQSR for ADN. 2D projections of TQSR are observed in 2 scenarios with DG penetration. The characteristics of TQSR are summarized.

The rest of the papers is organized as follows. The studied scenarios are introduced in Section II. The TQSR model is formulated in Section III. Section IV presents the case study. And the region map is discovered in Section V. Finally, Section VI draws the conclusion.

## II. SCENARIOS

For distribution systems, the region theory is mainly used in urban areas, where the ADN will be firstly developed. On one hand, the security-related problems in the urban distribution networks are usually more complicated than those in rural areas due to flexible switch operations [19] and high percentage of DGs. Thus, a new security assessment approach is urgently needed. On the other hand, the advanced secondary equipment and high-level automation of the urban distribution systems lay a basis for the application of the region

approach. Other features of the urban distribution systems include: ① the power supply range of the substation is relatively short; ② most buses and DGs are capable of regulating the bus voltage.

The DG penetration will affect the security feature of the distribution systems. Two kinds of DG penetrations are usually used, which are capacity penetration (CP) and power penetration (PP). CP is used to define the percentage of annual maximum hourly distributed generation and maximum hourly consumption of the system. And PP is used to define the percentage of the power provided by distributed generators and the power consumption of the system at a specific moment [20]. In this paper, only CP is discussed, which is defined as the ratio of the maximum DG capacity to summit the loads in the same area within one year.

According to different CPs, two typical scenarios for future ADN are studied in this paper, which are the high penetration supply network (HPSN) and very high penetration balanced network (VHPBN), respectively [21].

According to the concepts of HPSN and VHPBN as well as the effective planning schemes based on the definition in [22], it is referred that the CP of HPSN is around 40% and the power consumption of the load is received equally from the transmission system and local DGs. The CP of VHPBN is around 100% and all the power consumption of the load is from local DGs within a certain time. Compared with the traditional distribution network for load supply only (LSN), both HPSN and VHPBN are turned into the system with comprehensive service function of load supply and DG absorption.

Some assumptions are made in this paper according to the aforementioned features of the scenarios.

1) The approach of DC power flow [22] is utilized.

Firstly, the bus voltage profile is considered to be qualified. Both the system and the DGs are all able to regulate the bus voltage because the reactive power compensation equipment is sufficient and the voltage can be well controlled in the urban distribution networks. Even if the voltage profile has to be monitored, TQSR can be easily updated with the security voltage region (SVR) proposed in [23], because the intersection set can be made by different types of regions.

Secondly, the network loss can be included in the power flow of the feeder outlets [23], because the feeders are usually short in length and the network loss ratio is small in urban distribution networks.

Finally, it is shown in [9] that, compared with the accurate region using AC power flow, the error of security boundary calculation is acceptable for urban distribution networks when the DC power flow is used. In fact, the DC power flow is widely used in the existing researches on the security assessment of distribution networks such as DSSR [5], [11], [24], [25] and power supply capability [23]. It should be noted that some simple results based on AC power flow is also demonstrated in the case study as comparison.

2) Three-phase imbalance is neglected [5], [26], because the error is acceptable when a representative phase current is used in the security analysis.

3) The contingencies of DG are not considered.

### III. TQSR MODEL

#### A. Formulation

The TQSR model is compactly formulated as:

$$\Omega_{TQSR} = \left\{ W = (S_1, S_2, \dots, S_i, \dots, S_n), W \in \Theta \mid S_{i,A} \cap S_{i,B} \cap S_{i,C} \right\} \quad (1)$$

where  $\Omega_{TQSR}$  is the TQSR;  $W = (S_1, S_2, \dots, S_i, \dots, S_n)$  is the  $n$ -dimension operation point, which is defined as the minimum set of the state variables that can determine the security state of ADN;  $\Theta$  is the state space, which is defined as the set of all the possible operation points;  $S_{i,A}$  is the constraint of state space;  $S_{i,B}$  is the capacity constraint of branches and substation under normal operation state; and  $S_{i,C}$  is the  $N-1$  security constraint. The state variables include the following:

1) Power flow data: the voltage amplitude and the angle of each bus, and the power and network loss of all the branches.

2) Operation data: the switch state and the tap position of transformers and capacitors.

$S_i$  is the total apparent power of bus  $i$ . Considering that one bus is connected to only one object (load or DG),  $S_i$  can be expressed as:

$$S_i = \begin{cases} S_{Li} & i \in L \\ S_{Gi} & i \in G \end{cases} \quad (2)$$

where  $S_{Li}$  and  $S_{Gi}$  are the apparent power of the load and DG on the bus  $i$ , respectively;  $L$  is the load set; and  $G$  is the DG set. The direction is positive when the power flows out of bus  $i$  ( $S_i > 0$ ). Thus,  $S_{Li} \geq 0$  and  $S_{Gi} \leq 0$ .

For some large-scale networks, the dimension of the operation point can be reduced by merging some buses [27], [28], which is shown in the case study.

TQSR is defined as a closed set of all the  $N-1$  secure operation points in the state space of ADN. The physical meaning of TQSR is that all the operation status are secure within TQSR. And the status on the boundary is secure, while the status out of the region is insecure.

#### B. State Space Constraint

$S_{i,A}$  represents that the power of each bus should be kept in a reasonable range. For example, the load cannot exceed its capacity of distribution transformer and the DG output cannot exceed its generation capacity.  $S_{i,A}$  is formulated as:

$$\begin{cases} S_{Li}^{\min} \leq S_{Li} \leq S_{Li}^{\max} & i \in L \\ -S_{Gi}^{\max} \leq S_{Gi} \leq 0 & i \in G \end{cases} \quad (3)$$

where  $S_{Li}^{\max}$  and  $S_{Li}^{\min}$  are the maximum and minimum apparent power of load  $i$ , respectively, and the default value of  $S_{Li}^{\min}$  is 0; and  $S_{Gi}^{\max}$  is the capacity of DG  $i$ .

#### C. Normal Operation State Constraints

$S_{i,B}$  is formulated as:

$$\begin{cases} |S_{Bi}| = \left| \sum_{j \in \Omega_{Bi}} S_j \right| \leq c_{Bi} & \forall i \in B \\ |S_{Ti}| = \left| \sum_{j \in \Omega_{Ti}} S_j \right| \leq c_{Ti} & \forall i \in T \end{cases} \quad (4)$$

where  $S_{Bi}$  is the power of branch  $i$  and  $\Omega_{Bi}$  is the set of its downstream buses, and the term of downstream means the direction from a substation transformer towards its feeder ter-

terminal [29];  $c_{Bi}$  is the capacity of branch  $i$ ;  $B$  is the branch set;  $S_{Ti}$  is the power of substation transformer  $i$ ;  $\Omega_{Ti}$  is the set of its downstream buses;  $c_{Ti}$  is the capacity of substation transformer  $i$ ; and  $T$  is the transformer set.

The absolute value symbol in (4) is necessary for the constraints formulated for bidirectional power flow.

#### D. $N-1$ Security Constraint

##### 1) Definition

If a distribution system is  $N-1$  secure, it means that the load supply and DG absorption in the non-fault areas will not be interrupted without any overloading or off-limit voltages after any single contingency [5]. The  $N-1$  security criterion has been widely used in the distribution system planning and operation in some countries [30].

##### 2) Contingency set

The contingency set is defined as the set of all the contingencies that the operator concerns. The contingency set of LSN contains only two kinds of serious contingencies, which are substation transformer contingency and feeder outlet contingency [5], [7], [9]. This is based on the premise that the failures at feeder outlets are more likely to cause the overloading of the adjacent components than other branches of the feeders.

However, the premise of LSN is invalid when the bidirectional power flow is considered in ADN because the current could be large in the middle section of a feeder but very small in the feeder outlet. The contingency set in this case should include the failures of all the branches instead of the feeder outlets.

##### 3) System actions after contingency

When a fault occurs at a substation transformer, the load of the faulty transformer will be transferred to adjacent transformers in the same substation with bus-tie switches. If the adjacent transformers are still overloading, some loads will be transferred to other substations by tie-switch operations among feeders.

When a fault occurs at a feeder branch, the breaker at the feeder outlet will be open. Then, the non-fault area on the same feeders has to go through a short outage. After the fault is isolated, the faulty feeder and connected feeders will be reconfigured to restore the service of the non-fault area as much as possible within the security constraints. There are usually more than one feasible restoration schemes [29]. The scheme that maximizes the service restoration is used in this paper. Each of the backup feeders restores only one section of the whole faulted feeder. This scheme can balance the branch load after contingencies.

##### 4) DG dispatch after contingency

The DG dispatch strategies after system contingencies will affect the security of ADN.

The main dispatch strategies of DG include 3 types: grid-connected DG, grid-disconnected DG and island DG [27]. For all these three strategies, DGs can be regarded as negative loads when DC power flow is used.

The grid-connected DG is connected to the system after the system contingency. Thus, it can improve  $N-1$  security because it enlarges the feeder capacity equivalently [27].

The grid-disconnected DG will be disconnected from the

network when the fault occurs, then it could enlarge the outage area, which is negative for  $N-1$  security. This type of DG can be regarded as the zero-output grid-connected DG after the contingency.

IEEE 1547 standard encourages the power utility and consumers to realize the islanded DG with advanced technologies. For multiple contingencies such as  $N-2$  contingencies, some loads cannot be restored by the feeder power source with feeder switch operations. In this circumstance, the islanded DG is of great significance to improve the system reliability.

However, since only single contingency is considered in TQSR for the urban distribution networks with sufficient feeder links, a DG can always find a feeder as the power source after the system contingency by proper reconfiguration. Thus, the islanded DG is not adopted because the security is already guaranteed by system actions.

### 5) Formulation of $N-1$ security constraints

The  $N-1$  security constraints are formulated as:

$$\begin{cases} S_{t,c} & \forall \psi_k \in \Psi \\ |S_{B_i}(k)| = \left| \sum_{j \in \Omega_{B_i}(k)} S_j \right| \leq c_{B_i} & \forall i \in B, \psi_k \notin B \\ |S_{T_i}(k)| = \left| \sum_{j \in \Omega_{T_i}(k)} S_j \right| \leq c_{T_i} & \forall i \in T, \psi_k \notin T \end{cases} \quad (5)$$

where  $\Psi$  is the contingency set;  $\psi_k$  is the contingency  $k$ , which represents a single contingency of a branch or a substation transformer;  $S_{B_i}(k)$  and  $S_{T_i}(k)$  are the power of branch  $i$  and transformer  $i$  after contingency  $k$ , respectively;  $\Omega_{B_i}(k)$  and  $\Omega_{T_i}(k)$  are the sets of downstream buses of the branch  $i$  and transformer  $i$  after contingency  $k$ , respectively; and  $\psi_k \notin B$  and  $\psi_k \notin T$  denote that the calculations of the power flow of the faulty component are not needed.

After contingency  $k$ , the network will be reconfigured to restore the service of the non-fault area. The power flow of the branches and transformers could be changed.

In LSN, the constraints of the feeder outlet branch are modeled only because the feeder outlet always burdens larger currents than any other downstream sections. However, when the bidirectional power flow is considered in ADN, the constraints of each branch of DS must be modeled because it is uncertain which branch has the largest current.

### E. Comparison with Traditional DSSR Model

The proposed TQSR model and traditional DSSR model [11] are compared as follows.

#### 1) Range of state space

Since the traditional DSSR only considers the loads only and the bus power is always a positive number, the state space is located in the quadrant I. However, the state space of ADN can cover all the quadrants because the bus power can be either positive or negative with the DG.

#### 2) Formulation of normal operation state

In the traditional DSSR model, the constraints in normal operation state are usually neglected because the constraints on an operation point are stronger under  $N-1$  contingency

than those in normal operation state. However, the constraints of TQSR model in normal operation state could be stronger than  $N-1$  security and thus it must be formulated.

#### 3) Contingency set

The contingency set of DSSR model contains only substation transformer contingency and feeder outlet contingency. However, the contingency set of TQSR model must include the contingencies of all the branches.

#### 4) Security constraints

For TQSR model with bidirectional power flow, the constraints of each branch must be modeled and the absolute value symbols of the inequalities are necessary. For a traditional DSSR model with radial power flow, the constraints of the feeder outlet branch are modeled and the absolute value symbols are not needed.

## IV. CASE STUDY

The characteristics of TQSR are observed on a small 4-bus test system in 2 different scenarios including HPSN and VHPBN. In the case studies, the boundary equation is first calculated according to TQSR model (1)-(4). Then, it is projected onto the 2D subspace [7], [25]. Afterwards, the TQSR projections on 2D subspace are observed and the features of quadrant, shape and security of TQSR model are analyzed. The conclusion from the 4-bus test system is further verified in a large-scale practical case.

### A. Scenario 1: HPSN

In this scenario, the security region of LSN and power collection distribution network (PCN) will be used as a comparison. The main function of PCN is to collect and deliver the generation of DGs to the upper-level transmission system [31]. LSN and PCN can be regarded as the special ADN with the lowest and the highest DG penetrations, respectively, which are useful to explain how DG penetration affects the characteristics of the security region.

The 4-bus test system of ADN is used, as is shown in Fig. 1.  $B_i$  means the switch  $i$  and  $N_i$  means the node  $i$ . The LSN and PCN in the same scale are shown in Figs. S1 and S2 of Supplementary Material A. The data of the grids for case study are in Table I.

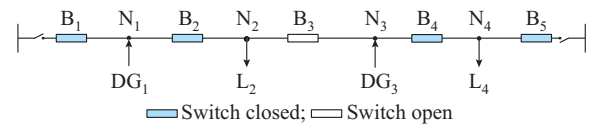


Fig. 1. 4-bus test system of ADN.

TABLE I  
BASIC DATA OF GRIDS FOR CASE STUDY

Grid	Branch capacity (MVA)	DG output range (MVA)	Load range (MVA)
AND	1	[-0.4, 1]	[0, 1.5]
LSN	1		[0, 0.8]
PCN	1	[-0.4, 0]	

The summit load of the ADN is 2 MVA. Thus, CP is

40%. It should be noted that each bus can be regarded as the sum of multiple DGs and loads. The security region characteristics can be clearly presented by a small case.

### 1) Boundary Equation

Considering the capacity constraints of the main transformer and the branch, the security boundary equations should be written and then simplified. The original equations of case grids are shown in Table SI of Supplementary Material A.

The physical meaning of all the security boundary equations is that the total actual power of the load and DGs carried by the branch shall be equal to the branch capacity.

According to the basic data of the grids for case study shown in Table I, the original security boundary equations can be simplified. The equations in red in Table SI are preserved and the final boundary equations of the three grids are shown in Table II.

TABLE II  
COMPARISON OF SECURITY BOUNDARY EQUATIONS OF GRIDS FOR CASE STUDY

Grid	Normal operation	$N-1$ security
ADN	$S_{L2}=1,  S_{L4}+S_{G3} =1$	$ S_{G1}+S_{L2}+S_{G3}+S_{L4} =1, S_{L4}=1,  S_{L4}+S_{G3}+S_{L2} =1$
LSN		$S_{L1}+S_{L2}+S_{L3}+S_{L4}=1$
PCN		$S_{G1}+S_{G2}+S_{G3}+S_{G4}=-1$

In Table II, it can be seen that compared with LSN/PCN, ADN has more boundary equations due to a larger contingency set and more branch constraints of TQSR model.

### 2) Quadrant

After observing the TQSR projections on 2D subspace, it can be concluded that TQSR can be located in any quadrant of the state space. The complete observation results are shown in Fig. S3-Fig. S15 of Supplementary Material A. The examples of quadrant IV are shown in Fig. 2.

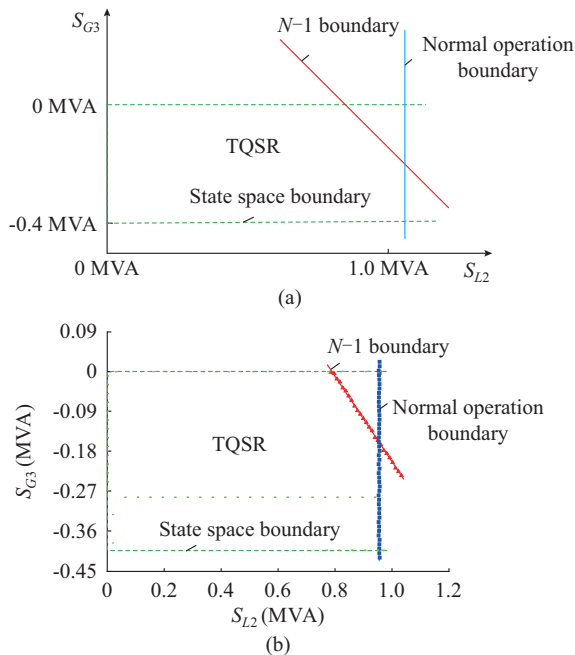


Fig. 2. Boundary figures using different power flow models. (a) DC power flow based model. (b) AC power flow based model.

In Fig. 2(a),  $S_{G3}$  and  $S_{L2}$  are observed and  $S_{G1}$  and  $S_{L4}$  are frozen at  $-0.4$  MVA and  $0.2$  MVA, respectively. It can be observed that TQSR is closed and bounded by  $N-1$  security boundary, normal operation boundary and state space boundary. If the security boundary is calculated by the AC power flow based model [10], the boundary figure is similar to Fig. 2. However, the boundary fluctuates around the straight line within a very small range, as shown in Fig. 2(b).

Table III shows the correspondence between the quadrant and observation variables. In Table III, the variables  $X$  and  $Y$  represent the two observation variables.

TABLE III  
RELATIONSHIP BETWEEN QUADRANT AND OBSERVATION VARIABLE

$X$	$Y$	Quadrant
Load	Load	I
DG	Load	II
DG	DG	III
Load	DG	IV

In Figs. S16-S20 of Supplement Material A, the region for LSN is located in quadrant I [5], [7] and the region for PCN is located in quadrant IV, which can be regarded as the special case of TQSR.

### 3) Shape Feature

According to the observation results of TQSR, the shape features of TQSR 2D projections can be included.

In general, 13 shapes can be observed in the 4-bus test system of HPSN according to the Figs. S3-S15 of Supplementary Material A. 2 shapes are the same as those of LSN and 11 shapes are newly added. Here, the same region figure in different quadrants will be counted as different shapes.

The 11 new shapes of TQSR can also be pentagon, ladder, rectangle or triangle, which is similar to those of traditional DSSR. The pentagon projection is shown in Fig. 2. These 11 new shapes contain the security boundary for positive power flow from the substation to its feeder terminal. The reason is that the CP of HPSN is around 40%, which means that the total capacity of DGs is usually less than the feeder capacity. Thus, the overloading caused by the reverse power flow (from a feeder terminal to the substation) will hardly occur.

However, the 11 new shapes of TQSR projections essentially differ from the traditional DSSR. They are not in quadrant I. Further, let  $\alpha$  be the angle between the inclined boundary and the coordinate axis towards the region, For the traditional DSSR,  $\alpha$  is always an acute angle (approximately 45), and it could be an obtuse angle (approximately 135) for TQSR.

Taking the pentagon in quadrant IV as an example, the comparison of traditional DSSR and TQSR as well as the angles between the inclined boundary and the coordinate axis is shown in Fig. 3.

This shape feature will lead to the difference of security feature between DSSR and TQSR, which will be illustrated in the following subsection.

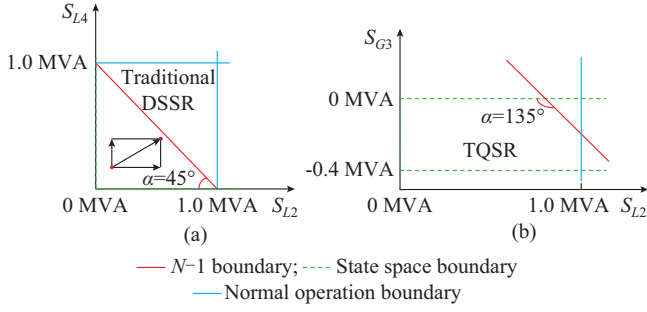


Fig. 3. Comparison of traditional DSSR and TQSR. (a) Triangle of traditional DSSR. (b) Pentagon of TQSR.

#### 4) Security

For the traditional DSSR, the most secure operation point is the original point (0, 0) [32], which represents that the total load of the system is zero. However, the most secure point will be changed in TQSR, which is corresponding to the maximum output of DGs and the zero loads. This is briefly illustrated in Fig. 4.

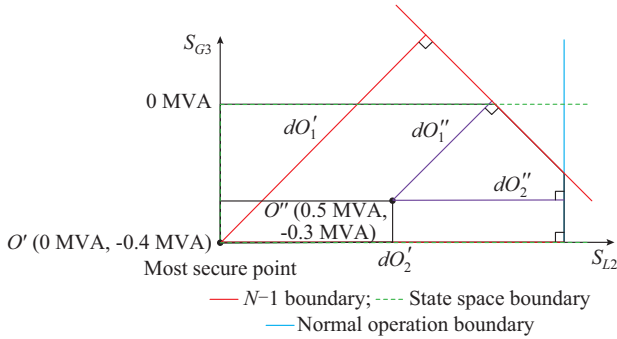


Fig. 4. Most secure operation point of TQSR of HPSN.

In Fig. 4, the security degree of operation point  $O''_2$  is lower than that of  $O'$ , because  $dO''_1 < dO'_1$ ,  $dO''_2 < dO'_2$ . Here,  $d$  is the security distance of an operation point to the effective security boundary [24]. Thus, the most secure point is  $O'$ . Also, even if the position of  $O'$  varies, the conclusion still remains unchanged.

Although the most secure point is changed, the general security principle of TQSR is the same as the traditional DSSR. In the traditional DSSR, the security degree decreases with the increasing load, which is called the monotone decreasing of the security [32]. The security degree decreases with the increasing cut-set payloads. The concept of the cut-set is shown in Fig. 5.

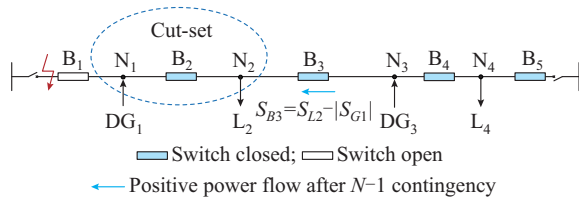


Fig. 5. Cut-set of DG and load.

In Fig. 5, the payload increases  $S_{L2} - |S_{G1}|$  and will reduce the remaining capacity of branch  $B_3$  after the contingency of

branch  $B_1$ .

Note that the increase of  $|S_{G1}| - S_{L2}$ , which is the reverse power flow, is always less than the capacity of  $B_3$ . Thus, for HPSN with 40% CP, it is always secure with the reverse power flow.

#### B. Scenario 2: VHPBN

TQSR of VHPBN is studied in this subsection and compared with TQSR of HPSN. The network topology of the 4-bus test system for VHPBN is the same as that of HPSN, except that the capacity of each DG is increased to 1.5 MVA. The summit load is 3 MVA, and CP is 100%.

##### 1) Boundary Equation

The boundary equations of VHPBN and HPSN are compared in Table IV.  $S_{G3} = -1$ ,  $S_{G1} = -1$ , and  $|S_{G1} + S_{L2} + S_{G3}| = 1$  are incremental equations of VHPBN.

TABLE IV  
COMPARISON OF BOUNDARY EQUATIONS OF VHPBN AND HPSN

Scenario	VHPBN	HPSN
Normal operation	$S_{L2} = 1, S_{G3} = -1$	$S_{L2} = 1$
$N-1$	$S_{G1} = -1, S_{L4} = 1,$ $ S_{G1} + S_{L2} + S_{G3}  = 1,$ $ S_{L4} + S_{G3} + S_{L2}  = 1,$ $ S_{G1} + S_{L2} + S_{G3} + S_{L4}  = 1$	$S_{L4} = 1,  S_{L4} + S_{G3} + S_{L2}  = 1,$ $ S_{L4} + S_{G3} + S_{L2} + S_{G1}  = 1$

In Table IV, 3 boundary equations are added for VHPBN compared with HPSN, because the branches adjacent to the DGs could be overloading in reverse power flow direction after the capacity of DG is improved. This will not occur when the DG penetration is 40%.

##### 2) Quadrant and Shape

The complete results of TQSR of VHPBN are shown in Fig. S1-S10 of Supplementary Material B.

Firstly, the quadrant feature of VHPBN is the same as that of HPSN. TQSR of VHPBN can be located in any quadrant of the state space.

Secondly, as to the shape feature, 24 shapes can be observed in the 4-bus test system of VHPBN. 12 shapes are the same as those of HPSN and another 12 shapes are newly added. Here, the same region figure in different quadrants will be counted as different shapes.

##### 1) Same shapes with HPSN

12 TQSR shapes of VHPBN are the same as those of HPSN, which can be pentagon, rectangle and triangle in different quadrants. The shapes in quadrant IV are shown in Figs. S1-S3 of Supplementary Material B.

In these shapes, only the positive  $N-1$  boundary exists because the level of the frozen loads is high and the frozen DG output is low. Thus, the branch overloading caused by the positive power flow occurs much more easily than that caused by the reverse power flow. Thus, the same shape region can be obtained.

##### 2) Different shapes from HPSN

12 TQSR shapes of VHPBN are different from those of HPSN, which can be divided into two types as follows.

Type 1: reverse shapes. There are 8 shapes in this type,

which is similar to HPSN. The projections can also be pentagon and rectangle, as is shown in Figs. S4 and S5 of Supplementary Material B. However, the orientation of the projections is different from HPSN. The pentagon projections in quadrant IV of HPSN and VHPBN are compared in Fig. 6 as an example.

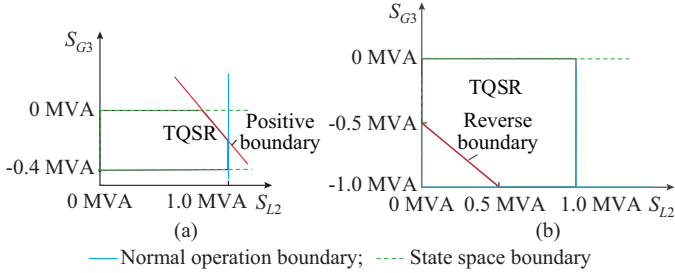


Fig. 6. Comparison of positive pentagon of HPSN and reverse pentagon of VHPBN. (a) Positive pentagon of HPSN. (b) Reverse pentagon of VHPBN.

In Fig. 6, the reverse security boundary rather than the positive security boundary exists in the TQSR projections. It is opposite to that of HPSN, which presents the positive security boundary. The main reason is that the level of the frozen loads is low while the frozen DG output is high. The branch overloading caused by the reverse power flow occurs more easily than the one caused by the positive power flow.

Type 2: shapes with double incline boundaries. 4 shapes of this type can be obtained. It is quite different from HPSN. The projections can be hexagon and new-type ladder. The hexagon projection in quadrant IV is shown in Fig. 7 and the ladder is shown in Fig. S7 of Supplement B.

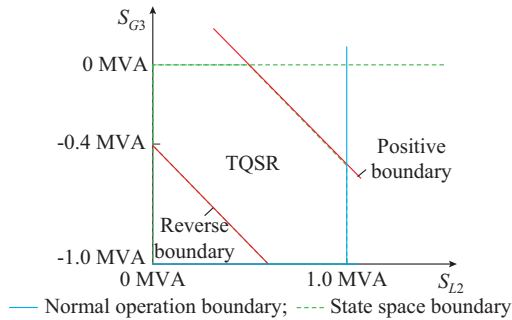


Fig. 7. Hexagon projection of TQSR on 2D subspace in quadrant IV of VHPBN.

In Fig. 7, both the positive and reverse boundaries (red incline boundaries) are presented to form the shape, which is the basic difference from HPSN and type 1 of VHPBN. The reason is that, when the DG output level of the frozen loads are moderate, the branch overloading could be caused by both the positive and reverse power flow.

### 3) Security

The security feature of VHPBN is different from that of HPSN.

1) The monotone decrease of the security holds for HPSN, which does not hold for VHPBN. For example, if VHPBN operates with the reverse power flow, the increase of bus power will reduce the reverse power flow and enlarge the security margin to the reverse boundary.

2) The most secure point for HPSN is corresponding to the maximum output of DGs and the zero loads, which should be original for VHPBN. It means that the load is zero or the DG output is zero. However, the requirement of original point is over-specific. If the operation point makes the cut-set power be zero, the point is also the most secure one. This is because the capacity of the branch adjacent to DGs is usually designed to be large enough to deliver the power generated by DGs. Thus, DG and its adjacent load can be regarded as a cut-set. For example, in Fig. 1, to guarantee the delivery of DG<sub>1</sub>, the capacity of B<sub>2</sub> will be large enough. Thus, DG<sub>1</sub> and L<sub>2</sub> can be regarded as one cut-set.

The security feature of TQSR for HPSN is based on an important premise. The total capacity of DGs on a feeder cannot exceed the feeder capacity (40% CP is consistent with the premise). However, in VHPBN, the capacity of total DGs with 100% CP could be larger than the feeder capacity and the security features will be different. The branch overloading could be caused by both positive and reverse power flows.

### C. Practical Case

A modified IEEE RBTS test system [33] is used to verify the characteristics in the 4-bus test system. The test system has three 110 kV substations, 6 substation transformers, 20 feeders and 104 buses as shown in Fig. 8. For HPSN, 14 buses containing DGs (white circle) are presented in Fig. 8. The total capacity of all DGs is 13.1 MVA, the summit load is 40 MVA, and CP is 40.5%. For VHPBN, 20 buses contain DGs, which are presented by 14 buses and 6 new-added buses (blue circle) in Fig. 8. The total capacity of DGs is 38.5 MVA, the summit load is 40 MVA, and CP is 96.25%.

The conclusion of the practical case is the same as the 4-bus test system. Due to the page limit, the complete results are shown in Supplementary Material C.

## V. REGION MAP

The region map is discovered based on the summary of the region characteristics of LSN, HPSN and VHPBN for the three grids with different DG penetrations, as shown in Fig. 9. Each symbol is marked with an ID below. In the ID, the first number means the quadrant. The alphabet represents the shape, in which T is triangle; L is ladder; P is pentagon; PL is parallelogram; and H is hexagon. “+” means the positive boundary exists in the shape and “-” means the negative boundary exists. The rectangle region does not contain decline boundary so that it does not need “+” or “-”.

### A. Feature of Region Map

In Fig. 9, it can be seen that all the 4 shapes in LSN also exist in HPSN. Besides, 12 new shapes are added in HPSN, which are highlighted with yellow color. Each quadrant (II, III, IV) provides 4 new shapes of HPSN because the region is expanded to all of quadrants from single quadrant. Besides, all the 16 shapes in HPSN also exist in VHPBN. 24 new shapes are added in VHPBN, which are highlighted with yellow color. Each quadrant (I-IV) provides 6 new shapes because the reverse boundary exists in VHPBN.

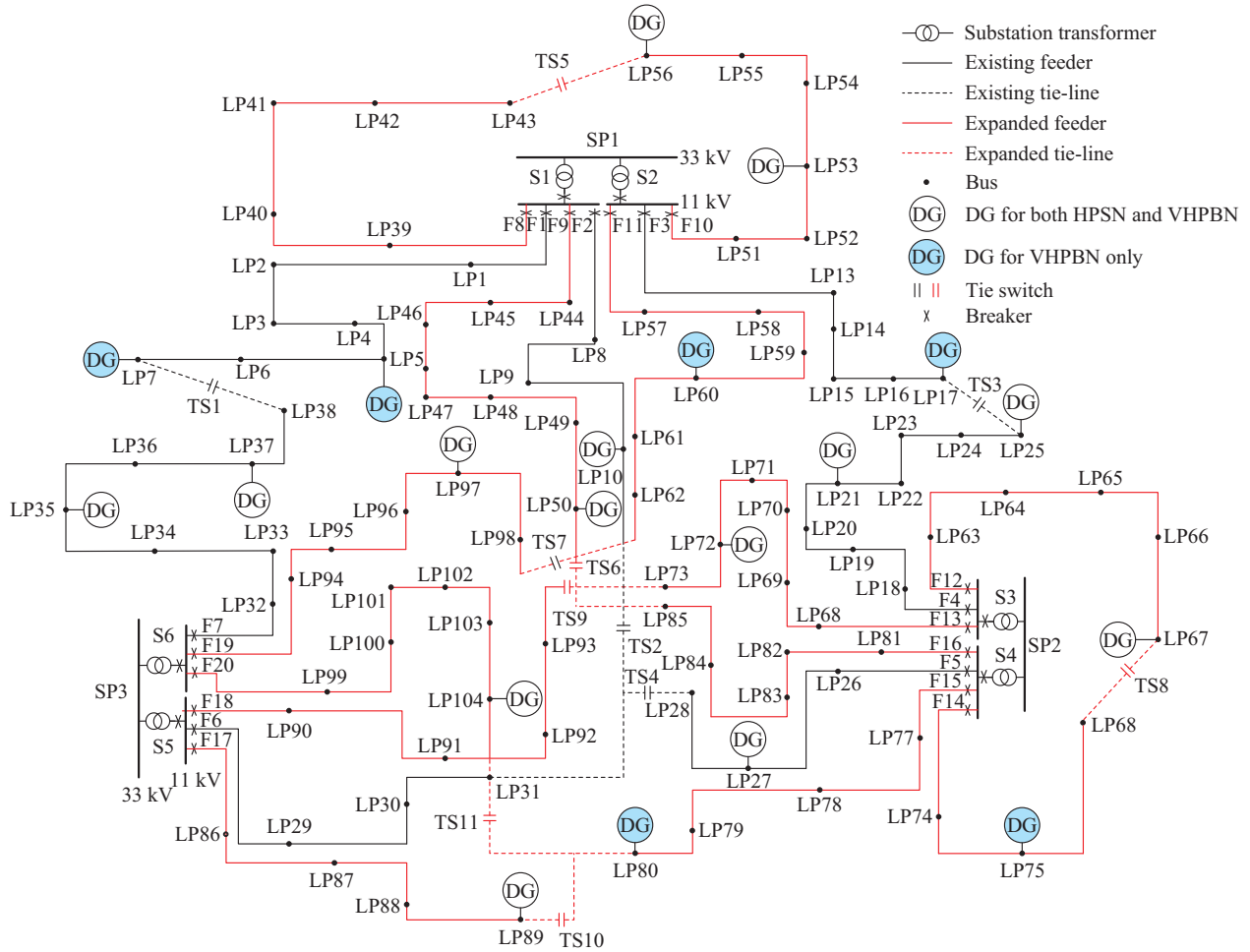


Fig. 8. A modified IEEE RBTS test system with DGs.

	Quadrant I				Quadrant II				Quadrant III				Quadrant IV				Total
LSN 0%																4	
HPSN 40%																	16
VHPBN 100%																	40

Fig. 9. Region map.

**B. Value of Region Map**

1) The region map summarizes the features of DSSR and TQSR and shows the maximum possible region shapes that a distribution system could have. For instance, the region of LSN has at most 4 shapes according to the map. The pentagon will never be obtained in any LSN. The region of HPSN has at most 4 shapes according to the map. The hexagon

will never be obtained in any HPSN.

In the 4-bus test system of HPSN, 13 shapes exist, all of which are included in the 16 shapes of HPSN in the region map. 3 shapes do not exist, whose ID are “1L+”, “1R” and “3L+”. In the 4-bus test system of VHPBN, 24 shapes exist, all of which are included in the 40 shapes of VHPBN in the region map. 16 shapes do not exist, whose ID are “1L+”,

“1H+−”, “1L+−”, “1L−”, “1PI+−”, “2L+”, “2L−”, “2PI+−”, “3L+−”, “3L+”, “3H+−”, “3PI+−”, “3L−”, “4L+”, “4L−”, “4PI+−”.

2) The region map can be used to categorize the distribution networks. For example, if a hexagon region projection is observed in quadrant IV, it can be found in the map that the system is a VHPBN.

## VI. CONCLUSION

This paper proposes the concept and model of TQSR for ADN. The 2D projections of TQSR are observed in 2 DG penetration scenarios. The characteristics of TQSR are summarized as follows.

1) Compared with the traditional DSSR, it is most obvious that TQSR is transformed from a single-quadrant region to a total-quadrant region.

2) For HPSN, at most 12 new shapes will be obtained in quadrants II, III and IV compared with those in LSN, including the triangle, ladder, pentagon and rectangle. For VHPBN, at most 24 new shapes in all quadrants will be obtained compared with HPSN, including the reverse triangle, reverse ladder, reverse pentagon, hexagon, parallelogram and ladder with both positive and reverse boundaries.

3) For HPSN, the most secure operation point is the one in which the DG output reaches the peak value and the power of the load is zero. For VHPBN, the most secure point is the original point or the point that makes the cut-set power be zero.

The region map is discovered to summarize the characteristic of TQSR and provide the maximum possible shapes that a region could have, which can also be used to categorize the distribution networks.

TQSR will be useful for the optimization problem and probabilistic assessment of ADN with plenty of uncertainties. Future work includes complete security region considering energy storage, microgrid and active load. More serious contingencies will also be studied such as weather conditions,  $N-2$  contingencies, and DG contingency.

## REFERENCES

- [1] D. A. Roberts and J. Scott, “Assessing future uncertainties on today’s distribution networks,” in *Proceedings of IET Conference on Power in Unity: a Whole System Approach*, London, UK, Oct. 2013, pp. 1-32.
- [2] Q. Shi, C. Chen, A. Mammoli *et al.*, “Estimating the profile of incentive-based demand response (IBDR) considering technical models and social-psychological factors,” *IEEE Transactions on Smart Grid*, vol. 11, no. 1, pp. 171-183, Jan. 2020.
- [3] S. Chowdhury, S. P. Chowdhury, and P. Crossley, *Microgrids and Active Distribution Networks*. London: The Institution of Engineering and Technology, 2009, pp. 15-33.
- [4] K. Morison, L. Wang, and P. Kundur, “Power system security assessment,” *IEEE Power & Energy Magazine*, vol. 2, no. 5, pp. 30-39, Sept. 2004.
- [5] J. Xiao, W. Gu, C. Wang *et al.*, “Distribution system security region: definition, model and security assessment,” *IET Generation, Transmission & Distribution*, vol. 6, no. 10, pp. 1029-1035, Oct. 2012.
- [6] F. Wu and S. Kumagai, “Steady-state security regions of power systems,” *IEEE Transactions on Circuits & Systems*, vol. 29, no. 11, pp. 703-711, Nov. 1982.
- [7] Y. Yu, H. Liu, and Y. Zeng, “Novel optimization method of transient stability emergency control based on practical dynamic security region (PDSR) of power systems,” *Science in China*, vol. 47, no. 3, pp. 376-382, Feb. 2004.
- [8] Y. Liu and Y. Yu, “Probabilistic steady-state and dynamic security assessment of power transmission system,” *Science China Technological Sciences*, vol. 56, no. 5, pp. 1198-1207, May 2013.
- [9] J. Xiao, L. Zuo, G. Zu *et al.*, “Model of distribution system security region based on power flow,” *Proceedings of the CSEE*, vol. 37, no. 17, pp. 4941-4949, Sept. 2017.
- [10] J. Xiao, G. Zu, X. Gong *et al.*, “Observation of security region boundary for smart distribution grid,” *IEEE Transactions on Smart Grid*, vol. 8, no. 4, pp. 1731-1738, Jul. 2017.
- [11] J. Xiao, G. Zu, X. Gong *et al.*, “Model and topological characteristics of power distribution system security region,” *Journal of Applied Mathematics*, vol. 2014, pp. 1-13, Jul. 2014.
- [12] I. Genc, R. Diao, V. Vittal *et al.*, “Decision tree-based preventive and corrective control applications for dynamic security enhancement in power systems,” *IEEE Transactions on Power Systems*, vol. 25, no. 3, pp. 1611-1619, Aug. 2010.
- [13] T. Jiang, H. Jia, Y. Jiang *et al.*, “Cutset-angle based wide area thermal security region and its application in china southern power grid,” *International Transactions on Electrical Energy Systems*, vol. 24, no. 11, pp. 1600-1617, Jan. 2015.
- [14] J. Xiao, G. Zu, Q. He *et al.*, “A new DMS with real-time security analysis and control based on security region,” in *Proceedings of PES General Meeting*, Denver, USA, Jul. 2015, pp. 26-30.
- [15] J. Liu, H. Cheng, Q. Xu *et al.*, “Stochastic planning of smart distribution network based on security distance methodology considering fault recovery,” *Automation of Electric Power Systems*, vol. 42, no. 5, pp. 64-71, Mar. 2018.
- [16] L. Yang, Y. Li, Z. Li *et al.*, “Energy rebalance control and safe operation region analysis of MMC with sub-module fault,” *Electric Power Automation Equipment*, vol. 38, no. 4, pp. 52-59, Apr. 2018.
- [17] H. Xiao, Z. Ye, F. Ma *et al.*, “Calculation and analysis of the safe operation boundary of shipboard DC zonal electric distribution system,” *Transactions of China Electrotechnical Society*, vol. 31, no. 20, pp. 202-208, Oct. 2016.
- [18] C. Wan, J. Lin, W. Guo *et al.*, “Maximum uncertainty boundary of volatile distributed generation in active distribution network,” *IEEE Transactions on Smart Grid*, vol. 4, no. 9, pp. 2930-2942, Jul. 2018.
- [19] D. M. Staszkesy, D. Craig, and C. Befus, “Advanced feeder automation is here,” *Power and IEEE Energy Magazine*, vol. 3, no. 5, pp. 56-63, Sept. 2005.
- [20] B. Zhao, X. Zhang, and B. Hong, “Energy penetration of large-scale distributed photovoltaic sources integrated into smart distribution network,” *Electric Power Automation Equipment*, vol. 32, no. 8, pp. 95-100, Aug. 2012.
- [21] J. Xiao, B. Zhang, J. Li *et al.*, “Research idea on high penetration renewable energy generations distribution system planning based on security boundary,” *Automation of Electric Power Systems*, vol. 41, no. 9, pp. 1-9, May 2017.
- [22] D. V. Hertem, J. Verboomen, K. Purchala *et al.*, “Usefulness of DC power flow for active power flow analysis with flow controlling devices,” in *Proceedings of 8th IEE International Conference on AC and DC Power Transmission*, London, UK, Mar. 2006, pp. 58-68.
- [23] J. Xiao, F. Li, W. Gu *et al.*, “Total supply capability and its extended indices for distribution systems: definition, model calculation and applications,” *IET Generation, Transmission & Distribution*, vol. 5, no. 8, pp. 869-876, Aug. 2011.
- [24] S. Chen, Q. Chen, Q. Xia *et al.*, “Steady-state security assessment method based on distance to security region boundaries,” *IET Generation, Transmission & Distribution*, vol. 7, no. 3, pp. 288-297, Mar. 2013.
- [25] W. Wei, F. Liu, and S. Mei, “Dispatchable region of the variable wind generation,” *IEEE Transactions on Power Systems*, vol. 30, no. 5, pp. 2755-2765, Sept. 2015.
- [26] T. Yang and Y. Yu, “Static voltage security region-based coordinated voltage control in smart distribution grids,” *IEEE Transactions on Smart Grid*, vol. 9, no. 6, pp. 5494-5502, Nov. 2018.
- [27] H. Liao, D. Liu, Y. Huang *et al.*, “Load transfer capability analysis considering interconnection of distributed generation and energy storage system,” *International Transactions on Electrical Energy Systems*, vol. 24, no. 2, pp. 166-177, Feb. 2014.
- [28] L. Jia, X. Qian, H. Cheng *et al.*, “Bi-level optimal renewable energy sources planning considering active distribution network power transfer capability,” *Transactions of China Electrotechnical Society*, vol. 32, no. 9, pp. 179-188, May 2017.
- [29] S. Adhikari, F. Li, Z. Wang *et al.*, “Constructive back-feed algorithm for online power restoration in distribution systems,” in *Proceedings of PES General Meeting*, Calgary, Canada, Jul. 2009, pp. 4170-4174.

- [30] E. Lakervi and E. J. Holmes, *Electricity Distribution Network Design*, London: The Institution of Engineering and Technology, 2003.
- [31] J. Yang, J. E. Fletcher, and J. O'Reilly, "Multiterminal DC wind farm collection grid internal fault analysis and protection design," *IEEE Transactions on Power Delivery*, vol. 25, no. 4, pp. 2308-2318, Oct. 2010.
- [32] J. Xiao, G. Zu, G. Bai *et al.*, "Mathematical definition and existence proof of distribution system security region," *Proceedings of the CSEE*, vol. 36, no. 18, pp. 4828-4836, Sept. 2016.
- [33] R. Billinton and S. A. Jonnavithula, "Test system for teaching overall power system reliability assessment," *IEEE Transactions on Power Systems*, vol. 11, no. 4, pp. 1670-1676, Nov. 1996.

**Jun Xiao** received the B.S., M.S. and Ph.D. degrees in electrical engineering from Tianjin University, Tianjin, China. In 2010, he was a Visitor Scholar in Department of Electrical Engineering and Computer Science, University of Tennessee, Knoxville, USA. He is now a Professor with the School of Electrical Engineering, Tianjin University. His research interests include planning and operation of smart distribution networks, distributed storage and design of microgrids, theory of complex networks.

**Guoqiang Zu** received the B.S. and Ph.D. degrees in electrical engineering

from Tianjin University, Tianjin, China. He was a visitor Ph.D. in the Department of Electrical Engineering and Computer Science of University of Tennessee, Knoxville, USA, in 2016. He is now an Engineer from State Grid Tianjin Electric Power Research Institute, Tianjin, China. He is also a joint Post-doctoral Fellow of Tianjin University. His research interests include planning, assessment and operation of smart distribution networks and urban energy internet.

**Huan Zhou** received the B.S. degree in electrical engineering from Tianjin University, Tianjin, China, in 2015. He is currently pursuing the M.Sc. degree in electrical engineering at Tianjin University. His main research interests include planning and operation of smart distribution networks, distributed storage.

**Xinsong Zhang** received the B.E. degree in electrical engineering from Xi'an University of Technology, Xi'an, China, in 2002, and the M.Sc. degree in electrical engineering from Xi'an Jiaotong University, Xi'an, China, in 2005. He joined the faculty of Nantong University, Nantong, China, in 2006. In 2013, he received the Ph.D. degree from Hohai University, Nanjing, China. He is currently an Associate Professor of the School of Electrical Engineering, Nantong University. His research interests include power system operation and planning, wind power integration and energy storage systems.